agronomy

MDPI

Article

Biochar Increases Rice Yield in Soda Saline-Alkali Paddy Fields by Improving Saline-Alkali Stress and Phosphorus Use Efficiency

Xuebin Li †, Weikang Che †, Junlong Piao †, Yang Song, Xudong Wang, Yue Zhang, Shihao Miao, Hongyue Wang, Liming Xie, Jiayi Sun and Feng Jin *

Agronomy College, Jilin Agricultural University, Changchun 130118, China; lixuebin91666@163.com (X.L.); 13154369230@163.com (W.C.); ppp2147353805@163.com (J.P.); songyang19991017@126.com (Y.S.); wangxudong92@126.com (X.W.); 15044554600@163.com (Y.Z.); miaoshihao2024@163.com (S.M.); 15500279917@163.com (H.W.); 15043632826@163.com (L.X.); 15500407467@163.com (J.S.)

* Correspondence: jinfeng@jlau.edu.cn

† These authors contributed equally to this work.

Highlights:

- Biochar and phosphate fertilizers combined to alleviate soda saline-alkali barriers.
- Addition of biochar decreased the rice Na^+ concentration and Na^+/K^+ ratio in a soda saline-alkali paddy.
- Biochar enhances the efficiency of phosphate fertilizer utilization under soda saline-alkali stress.

Abstract: Soda saline-alkali significantly hinders rice growth, phosphorus utilization efficiency, and yield formation. The application of biochar can alleviate the adverse effects of saline-alkali stress on crops. However, there is limited research on the interaction between biochar and phosphorus fertilizer concerning ionic accumulation, phosphorus utilization efficiency, and rice yield in soda saline-alkali soils. A two-year field experiment was conducted to study the combined effects of biochar and phosphate fertilizer on ionic accumulation, physiological status, phosphorus utilization efficiency, and rice yield in soda saline-alkali soil. Four treatments were established for the study: NK (225 kg N, 75 kg K ha^{-1} $year^{-1}$), NPK (225 kg N, 70 kg P, 75 kg K ha^{-1} $year^{-1}$), NK + B [225 kg N, 75 kg K ha^{-1} $year^{-1}$, 1.5% biochar (w/w)], and NPK + B [225 kg N, 70 kg P, 75 kg K ha^{-1} $year^{-1}$, 1.5% biochar (w/w)]. The findings indicated that the combined application of biochar and phosphorus fertilizer (NPK + B) significantly reduced the Na^+ concentration, Na^+/K^+ ratio, malondialdehyde (MDA), superoxide anion (O_2^-), and hydrogen peroxide (H_2O_2) levels in rice plants. Furthermore, it resulted in a significant increase in K^+ concentration and elevated the levels of superoxide dismutase (SOD), peroxidase (POD), catalase (CAT), ascorbate peroxidase (APX), proline (Pro), soluble protein (SP), soluble sugar (SS), and acid phosphatase (ACP). The NPK + B treatment exhibited a significant difference compared to the other treatments ($p < 0.05$). Compared with NK, phosphorus accumulation and phosphorus utilization efficiency under NPK + B were significantly increased ($p < 0.05$). The average of biomass yield, grain yield, and harvest index of NPK + B, NK + B, and NPK significantly surpassed those of NK by 6.28–12.25%, 19.80–42.13%, and 11.59–24.64%, respectively. Moreover, a significant difference was observed between NPK + B and the other treatments ($p < 0.05$). Principal component analysis of the two-year mean data revealed a strong positive correlation of 89.5% for PC1 and a minor negative correlation of 4.4% for PC2. Our research findings demonstrate that the combination of biochar and phosphorus fertilizer effectively enhances salt and alkali tolerance in rice plants, resulting in increased yield through improved ionic balance and physiological status.

Keywords: soda saline-alkali stress; biochar; ionic balance; phosphorus use efficiency; rice

check for updates

Citation: Li, X.; Che, W.; Piao, J.; Song, Y.; Wang, X.; Zhang, Y.; Miao, S.; Wang, H.; Xie, L.; Sun, J.; et al. Biochar Increases Rice Yield in Soda Saline-Alkali Paddy Fields by Improving Saline-Alkali Stress and Phosphorus Use Efficiency. *Agronomy* **2024**, *14*, 2159. https://doi.org/10.3390/agronomy14092159

Academic Editors: David Houben and Stephan M. Haefele

Received: 1 August 2024
Revised: 13 September 2024
Accepted: 19 September 2024
Published: 21 September 2024

1. Introduction

The soda saline-alkali land in the western region of the Songnen Plain in Northeast China is one of the three principal distribution areas of soda saline-alkali land globally,

covering approximately 3.42 million hectares [1]. Soda saline-alkali soil is characterized by high levels of Na_2CO_3 and $NaHCO_3$, contributing to its high soluble salt content, strong alkalinity, strong dispersion, poor permeability, weak structure, and low fertility. Saline-alkali soils primarily hinder crop development by inducing osmotic stress, ionic toxicity, oxidative stress, and nutrient imbalances [2,3]. The high salt content in saline-alkali soils restricts plants' ability to absorb essential nutrients and water, leading to osmotic stress [4]. The accumulation of Na^+ within both the inner and outer plant cells during saline-alkali stress disrupts the balance of sodium and potassium ions in the cytoplasm, resulting in ionic toxicity [5,6]. Moreover, plants under this stress generate increased levels of reactive oxygen species (ROS), leading to cell wall disruption and oxidative damage [7]. Simultaneously, high pH directly harms plant roots, affecting their tissue structure and nutrient absorption [8,9]. The soil soda saline-alkali barrier has now become the most critical factor limiting agricultural development and crop yield improvement in the Songnen Plain.

Phosphorus is an essential element for plant growth and development, playing a significant role in plant nutrition, soil fertility, and ecosystem productivity [10]. In saline-alkali soils, excessive soluble salts and exchangeable sodium can hinder phosphorus uptake and utilization by competing with essential nutrient isotopes [11]. Furthermore, soda saline-alkali soils are characterized by high levels of CO_3^{2-} and HCO_3^-, which can react with available phosphorus to form insoluble calcium phosphate salts, further reducing the availability of phosphorus [12,13]. Previous research has shown that in high salinity, alkalinity, and pH environments, soil aggregates disperse significantly, and the decomposition of organic matter occurs at an accelerated rate. This phenomenon results in increased leaching of mineral nutrients, and phosphorus in particular [14]. Simultaneously, the internal stability of soil microbial cells is disrupted, affecting the breakdown of phosphates and soil organic matter, which consequently influences the transformation of phosphorus and its uptake and utilization by plants [15,16]. Negative effects such as ion toxicity, osmotic stress, oxidative stress, and high pH can significantly inhibit the growth and physiological function of plant roots, resulting in a marked reduction in phosphorus uptake and utilization [17,18]. Additionally, these factors can damage the structure of the plasma membrane, decrease chlorophyll content and photosynthetic rates, and adversely affect phosphatase activity, assimilation, and transport efficiency [19,20]. Therefore, it is essential to tackle soda saline-alkali stress and improve phosphorus absorption and utilization efficiency in rice under these conditions to enhance rice yields in soda saline-alkali paddy soils.

Biochar possesses physical and chemical properties, including a high specific surface area, stability, porosity, and adsorption capacity. It has played a significant role in soil restoration and has been widely researched and applied in the agricultural sector in recent years [21]. Previous research has demonstrated that applying 1% biochar to saline soils in lightly and moderately dry fields in northwest China can promote Na^+ leaching, improve soil structure, and ultimately increase the concentration of inorganic phosphorus in the soil [22,23]. Strelko and Chintala demonstrated that biochar contains a portion of phosphorus that can be directly released into the root zone [24,25]. Moreover, due to its large surface area and adsorption capacity, biochar effectively reduces phosphorus leaching in the soil, thereby enhancing the uptake and utilization of phosphorus by crops. Previous research has shown that biochar has the potential to lower soil pH, enhance soil organic matter and dissolved organic carbon, and stimulate humus release, ultimately leading to improved phosphorus availability and increased wheat yield in salt-affected soils [26,27]. Liu et al. [28] discovered that the application of FeO^--modified biochar significantly increased both the organic carbon content and the relative abundance of phoD (alkaline phosphatase) bacteria in coastal saline-alkali soils. This enhancement facilitated the mineralization rate of soil organic phosphorus, ultimately improving phosphorus availability in coastal saline-alkali soils. Numerous studies have confirmed that applying biochar in saline-alkali soils can improve root zone conditions during salt stress, alter root structure and function, and significantly enhance the capacity for root phosphorus uptake [14,29,30]. Farhangi-Abriz demonstrated that the application of biochar significantly reduced oxida-

tive stress in bean plants under salt stress and promoted their adaptability to both salt and alkali conditions [31]. Our previous studies have shown that applying peanut shell biochar to heavily soda saline-alkali paddy fields significantly improved soil physical structure and saline-alkali characteristics [32–34]. Furthermore, it reduced Na^+, proline, and malondialdehyde levels in rice tissues, increased K^+ concentration in the leaves, and enhanced both biomass production and grain yield in rice [35,36]. However, the mechanism by which biochar regulates phosphorus uptake and use efficiency in rice under severe soda saline-alkali conditions has not been systematically reported.

Our study hypothesized that biochar application can alleviate soda saline-alkali stress, regulate leaf physiology, and improve phosphorus utilization efficiency and yield in soda saline-alkali paddy soils, while also clarifying the underlying mechanisms. Therefore, this study was conducted to evaluate the effects of combined biochar and phosphate fertilizer application on ionic accumulation, antioxidant enzyme activity, osmotic regulator concentration, cell membrane permeability, acid phosphatase concentration, and the absorption, transport, and utilization of phosphorus in rice grown in soda saline-alkali paddy soils. Additionally, the study aimed to clarify the physiological mechanisms behind the impacts of the combined application on phosphorus absorption and utilization efficiency and on the yield of rice in these soils. The findings provide a theoretical foundation for using biochar to enhance the sustainability of rice cultivation in soda saline-alkali soils.

2. Materials and Methods

2.1. Study Site and Experimental Soil Properties

During 2022 and 2023, field experiments were conducted at the Saline-Alkali Research Base of Jilin Agricultural University, Da'an City, Jilin Province, China (45°35′ N, 123°50′ E). The average annual sunshine hours at the test site were 2915 h, the average annual temperature was 4.69 °C, the average annual precipitation was about 415.49 mm, and the average evaporation was about 1697.11 mm. According to the International Society of Soil Sciences, the soil is classified as saline-alkali with a clayey loam texture, comprising 23.13% sand, 38.14% loam, and 37.60% clay. The basic physicochemical properties of the soil (0–20 cm) were measured before the experiment, and the relevant indices are presented in Table 1.

Table 1. The initial physicochemical properties of the experimental soil (0–20 cm).

Soil Properties (0 to 20 cm Soil Layers)	Value
Sand content (%)	23.13 ± 1.11
Silt content (%)	38.14 ± 1.31
Clay content (%)	37.60 ± 2.09
Bulk density (g cm^{-3})	1.61 ± 0.02
ECe (μs m^{-1})	24.08 ± 0.71
pH	10.10 ± 0.24
SARe (mmolc $L^{-1})^{1/2}$	368.11 ± 14.03
CEC (cmolkg^{-1})	10.99 ± 0.34
ESP (%)	71.11 ± 2.17
Organic matter (g kg^{-1})	0.64 ± 0.04
Total N (g kg^{-1})	0.27 ± 0.11
Alkali-hydrolyzable N (mg kg^{-1})	16.30 ± 1.11
Available P (mg kg^{-1})	9.13 ± 0.68
Available K (mg kg^{-1})	107.25 ± 5.68

ECe electrical conductivity of soil saturation extract, SARe sodium adsorption ratio of soil saturation extract, CEC cation exchange capacity, ESP exchangeable sodium percentage, N nitrogen, P phosphorus, K potassium. Values are means ± SD.

2.2. Experimental Design and Field Management

A two-year field trial was conducted in 2022 and 2023, using a randomized block design with four treatments and three replicates. The treatments included NK (225 kg N, 75 kg K ha^{-1} $year^{-1}$), NPK (225 kg N, 70 kg P, 75 kg K ha^{-1} $year^{-1}$), NK + B [225 kg N,

75 kg K ha^{-1} $year^{-1}$, 1.5% biochar (*w*/*w*)], and NPK + B [225 kg N, 70 kg P, 75 kg K ha^{-1} $year^{-1}$, 1.5% biochar (*w*/*w*)]. The biochar dosage was calculated as 1.5% (*w*/*w*) based on the weight ratio of biochar to the tillage layer (expressed as B). Each test plot covered an area of 25 m^2 (5 m × 5 m) and was separated by a 50 cm wide aisle. Additionally, each plot was equipped with an independent irrigation and drainage system. The rice variety selected for this field study was Changbai 9 (*Oryza sativa* L.), an elite cultivar recognized for its adaptability to saline-alkali paddy soils in Northeast China. Rice seeds were initially sown in a greenhouse on 12 April 2022, and 15 April 2023, and were subsequently transplanted to the paddy field on 22 May and 25 May, respectively. The transplantation density was established at 30 cm × 16.5 cm per hill, with three seeds planted per hill. The rice plants were ultimately harvested on 1 October 2022 and 3 October 2023. Biochar was applied once a year in the spring during land preparation.

2.3. Preparation of Biochar

Biochar was synthesized from peanut shells via a vertical kiln, supplied by Jinhefu Agricultural Development Company in Liaoning Province, China, under pyrolysis conditions of 550 °C for a duration of 4 h. The physicochemical characteristics of the biochar and peanut shells are detailed in Table 2. During the springs of 2022 and 2023, the biochar was evenly applied to the surface of the saline soil before rice transplanting and then incorporated into the topsoil (0 to 20 cm depth) using a wooden rake.

Table 2. Basic properties of raw peanut shell and biochar.

pH and Elemental Component	Peanut Shell	
	Raw Material	**Biochar**
pH	5.56 ± 0.11	7.94 ± 0.32
CEC (cmol kg^{-1})	-	78.69 ± 11.32
EC (dS m^{-1})	-	7.88 ± 0.59
C (mg g^{-1})	429.19 ± 13.05	540.64 ± 26.58
N (mg g^{-1})	10.85 ± 0.61	15.93 ± 1.01
S (mg g^{-1})	2.58 ± 0.05	6.85 ± 0.34
P (mg g^{-1})	0.29 ± 0.00	0.74 ± 0.03
Mg (mg g^{-1})	1.46 ± 0.01	0.25 ± 0.00
K (mg g^{-1})	5.51 ± 0.21	12.53 ± 0.51
Ca (mg g^{-1})	6.32 ± 0.43	2.01 ± 0.02
Na (mg g^{-1})	1.79 ± 0.39	1.17 ± 0.21

CEC cation exchange capacity, EC electrical conductivity, C carbon, N nitrogen, S sulfur, Mg magnesium, P phosphorus, K potassium, Ca calcium, Na sodium.

2.4. Sampling and Measurements

2.4.1. Measurement of Ionic Concentration in Plant Organs

At maturity, 15 rice plants were harvested from each treatment. The biomass was then separated into three components: stem-sheath, leaf, and panicle. These components were dried to a constant weight in an oven at 70 °C and ground into a powder. The samples were digested with 1% nitric-perchloric acid [37]. The concentrations of Na^+ and K^+ were determined using the flame photometer method (M410, Sherwood Scientific Ltd., Cambridge, UK), and the Na^+/K^+ ratio was subsequently calculated.

2.4.2. Measurement of Leaf Proline (Pro), Soluble Protein (SP), and Soluble Sugar (SS) Concentration

During the two growth stages, known as the full heading stage and the grain filling stage, nine representative rice plants were selected from each treatment, and the flag leaves of these plants were used for the analysis of relevant physiological indicators. The leaf bases and tips were removed, flash-frozen in liquid nitrogen, and stored in a −80 °C freezer for future use.

The proline concentration (Pro, μg g^{-1} FW) in fresh leaves was determined following the method described by Bates et al. [38]. Fresh leaf samples were mixed with a 3% solution of sulfosalicylic acid. A mixture of glacial acetic acid and acidic ninhydrin was subsequently added to the leaf sample solution in a test tube before incubation. Toluene was then introduced into the reaction mixture and allowed to sit in the dark at room temperature for 20 min, after which the absorbance of the toluene was measured spectrophotometrically. Soluble protein concentration was determined using Coomassie Brilliant Blue G-250 as described by Bradford et al. [39]. Fresh samples were ground and centrifuged using a mortar and pestle. Brilliant Blue G-250 was added, and the absorbance was measured at 595 nm. The SS concentration of cotyledons was measured using anthrone colorimetry, following the method outlined by Du et al. [40]. Fresh leaf samples were ground and mixed with 80% ethanol, then shaken and placed in a water bath. After centrifugation, the supernatant was transferred to a 10 mL centrifuge tube. The precipitate was extracted two additional times with an 80% ethanol solution. Subsequently, it was combined with anthrone reagent, boiled, and cooled in a water bath. The absorbance at 620 nm was then measured using a spectrophotometer.

2.4.3. Measurement of Leaf Malondialdehyde (MDA), Superoxide Anion (O_2^-), and Hydrogen Peroxide (H_2O_2) Concentration

The MDA concentration was measured using the thiobarbituric acid method as outlined by Stewart et al. [41]. Approximately 1.0 g of the sample was weighed, then mixed with 10% trichloroacetic acid (TCA) and homogenized through centrifugation. The supernatant was collected and combined with 0.6% thiobarbituric acid, followed by boiling in a water bath. After cooling, the mixture was centrifuged again. Absorbance was measured at 532, 600, and 450 nm. The O_2^- concentration (μg g^{-1} FW) was measured following the method outlined by Wang et al. [42]. The samples were homogenized with 65 mmol L^{-1} phosphate buffer and then centrifuged. The resulting supernatant was mixed with phosphate buffer and hydroxylamine hydrochloride solution and incubated. Next, p-aminobenzene sulfonic acid and α-naphthylamine were added sequentially. The reaction mixture was incubated at 30 °C for 30 min with shaking. Chloroform was added in equal volume to extract the pigment, followed by centrifugation, and the absorbance was measured at 530 nm. The H_2O_2 concentration (μmol g^{-1} FW) was quantified following the protocol outlined by Velikova et al. [43]. Approximately 0.5 g of the sample was homogenized in TCA, then ground and centrifuged. The supernatant was mixed with phosphate buffer and potassium iodide, and absorbance measurements were taken at 390 nm.

2.4.4. Measurement of Leaf Superoxide Dismutase (SOD), Peroxidase (POD), Catalase (CAT), Ascorbate Peroxidase (APX), and Acid Phosphatase (ACP) Concentration

Fresh leaf samples were collected and milled for enzyme activity analysis. SOD activity was measured using the nitroblue tetrazolium (NBT) method at a wavelength of 560 nm, where a 50% inhibition of NBT reduction corresponded to one unit of enzyme activity (u), expressed as (μg^{-1} FW). POD activity was assessed by the change in absorbance at 470 nm, with one unit of enzyme activity (u) defined as an OD470 change of 0.01 per minute per unit FW [44]. Catalase activity was assessed by measuring the change in absorbance at 240 nm, with one unit of enzyme activity (u) defined as a 0.1 decrease in OD240 over the course of one minute. Ascorbate peroxidase activity was determined by monitoring the decrease in absorbance at 290 nm and expressed as (μg^{-1} FW) [45]. Acid phosphatase activity was evaluated using a kit from Beijing Solaibao Technology Co., Ltd. (Beijing, China). The procedure involved homogenizing approximately 0.1 g of fresh tissue sample with 1 mL of extraction solution, followed by centrifugation. The resulting supernatant was then mixed with the reagents according to the instructions and measured for absorbance at 510 nm.

2.4.5. Measurement of Phosphorus Concentration in Plants

The rice plants were sampled at different growth stages, including tillering, jointing, heading, filling, and maturity. Fifteen rice plants were harvested from each treatment; the root systems were removed, and the aboveground parts were divided into leaves, stem-sheath, and spikes. The fresh weight of each part was measured, followed by drying in an oven at 105 °C for 30 min and then at 70 °C until a constant weight was reached. The dry matter weight of leaves, stem-sheath, and ears at each stage was determined using an analytical balance. Subsequently, each sample was minced, digested with H_2SO_4 and 30% H_2O_2, and phosphorus (P) was measured using an ultraviolet-visible spectrophotometer (TU-1900, Beijing Puxi General Instrument Co., Ltd., Beijing, China). The formula for plant phosphorus accumulation and use efficiency is described in [19].

$$\text{PA (kg ha}^{-1}) = \text{DW} \times \text{P content}$$

$$\text{PT (kgha}^{-1}) = \text{P content at heading} - (\text{stem sheath and leaf}) \text{ P content at maturity}$$

$$\text{PUE (\%)} = (P_P - P_0) \times 100/\text{FP}$$

$$\text{PHI (\%)} = (\text{grain P at maturity} - \text{total P content of above ground at maturity}) \times 100$$

$$\text{PAE (kg kg}^{-1}) = (Y_P - Y_0) \times 100/\text{FP}$$

$$\text{PFP (kg kg}^{-1}) = Y_P/\text{FP}$$

$$\text{Phosphorus absorption efficiency (\%)} = \text{P content at maturity} \times 100/\text{FP}$$

$$\text{P increment amount in panicle (kg ha}^{-1}) = \text{grain P at maturity} - \text{grain P at heading}$$

where PA represents the accumulation of phosphorus in the plant (kg ha^{-1}), DW represents dry matter weight, P content represents phosphorus concentration in the stem sheath and leaves, and PT represents phosphorus transport in the stem sheath and leaves. PUE represents phosphorus utilization efficiency, PHI represents phosphorus harvest index, PAE represents phosphorus agronomic efficiency, and PFP represents phosphorus fertilizer partial productivity. P_P is the phosphorus absorbed by the plant with phosphorus application, P_0 is the phosphorus accumulation in rice without phosphorus application (NK treatment), and FP is the total amount of applied phosphorus (70 kg P ha^{-1} $year^{-1}$). Y_P is the rice yield in the phosphorus application area (NPK and NPK + B treatment), and Y_0 is the rice yield in the non-phosphorus application area (NK treatment).

2.4.6. Measurement of Rice Biomass Yield (BY), Grain Yield (GY), and Harvest Index (HI)

During the rice maturation stage, 15 rice plants were harvested from each treatment. After removing the roots, the plants were dried in an oven at 70 °C until they reached a consistent weight. The biomass of the plants was then recorded. From each trial plot, all rice plants within a 5 m^2 area were collected, and the rice yield was determined after threshing. The harvest index (HI) was computed by dividing the grain yield by the biomass yield.

2.5. Data Analysis

The SPSS 18.0 software (IBM Corp., Armonk, NY, USA) was utilized for data analysis according to the experimental design. Descriptive statistics were employed to assess the mean and standard deviation of the measured parameters. A one-way ANOVA was performed to evaluate the effect of biochar on related measured parameters, while a two-way ANOVA was used to assess the interaction between biochar treatment and year. The least significant difference (LSD) test was used to determine significant differences between treatments, with a significance level set at $p < 0.05$. Principal component analysis (PCA), Pearson correlation analysis, and figure generation were conducted using Origin Pro 2022 (Origin Lab Inc., Northampton, MA, USA).

3. Results

3.1. Concentrations of Sodium, Potassium Ions, and Sodium-Potassium Ratios in Leaves, Stem-Sheath, and Panicles

Figure 1 indicates that the addition of biochar (NK + B and NPK + B) resulted in a significant decrease in Na^+ concentration and the Na^+/K^+ ratio across all plant parts, while also showing an increase in leaf K^+ concentration ($p < 0.05$). Compared with NK, the average Na^+ concentration in the leaves, stem-sheath, and panicle under NPK + B, NK + B, and NPK treatments significantly decreased by 17.14–41.46%, 5.26–11.91%, and 5.90–17.68% (Figure 1A), respectively. The Na^+/K^+ ratio in different organs of rice followed the order of NPK + B < NK + B < NPK < NK over these two experimental years (Figure 1C). The difference between all the treatments reached a significant level ($p < 0.05$). Moreover, the average K^+ concentration in leaves increased by 78.84%, 36.48%, and 56.75% for the NPK + B, NK + B, and NPK treatments, respectively (Figure 1B), compared to NK, with all treatments differing significantly from the NK treatment ($p < 0.05$). All the treatments showed a similar effect in the stem-sheath and panicle. Additionally, the concentration of Na^+ in leaves was significantly lower in 2023 than in 2022, while the K^+ concentration in 2023 was significantly higher than that in 2022.

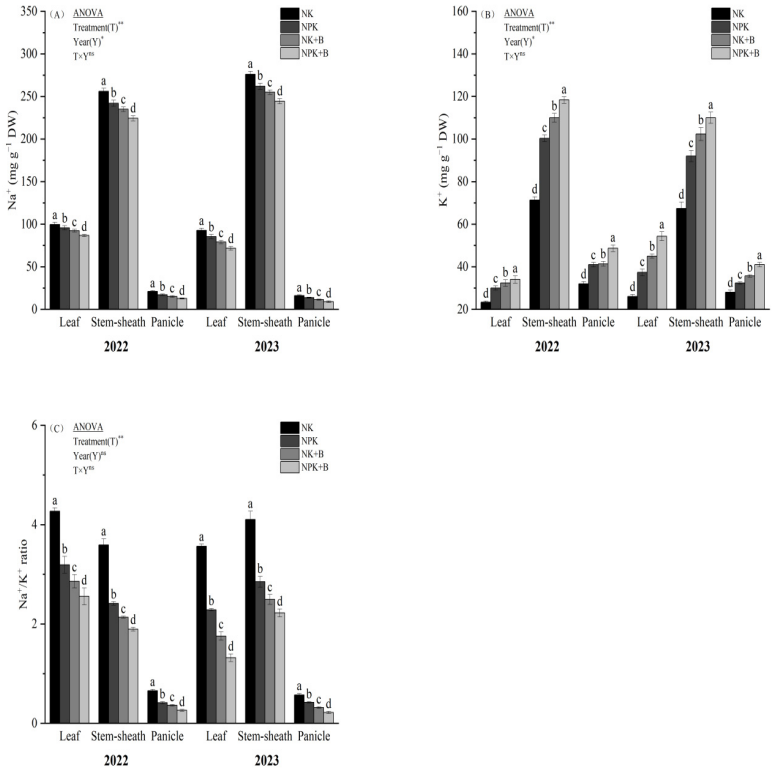

Figure 1. Effect of biochar combined with phosphorus on Na^+ (**A**), K^+ (**B**), and Na^+/K^+ ratio (**C**) in different rice organs. NK (225 kg N, 75 kg K ha^{-1} $year^{-1}$), NPK (225 kg N, 70 kg P, 75 kg K ha^{-1} $year^{-1}$), NK + B [225 kg N, 75 kg K ha^{-1} $year^{-1}$, 1.5% biochar (w/w)], and NPK + B [225 kg N, 70 kg P, 75 kg K ha^{-1} $year^{-1}$, 1.5% biochar (w/w)]. Note: ns, not significant; * and **, significant at $p < 0.05$ and $p < 0.01$. Different letters indicate significantly different values ($p < 0.05$).

3.2. Leaf Pro, SP, and SS Concentration

The impact of biochar and phosphorus fertilizer on the levels of Pro, SP, and SS in soda saline-alkali rice over two years is shown in Figure 2. Compared with NK, the average Pro concentrations of NPK + B, NK + B, and NPK at the heading stage increased by 22.75%, 13.89%, and 8.85%, respectively, while the average Pro concentrations at the filling stage increased by 19.93%, 10.56%, and 8.34%, respectively (Figure 2A). The difference between NPK + B and other treatments reached a significant level ($p < 0.05$). SP concentration showed

a trend of NPK + B > NK + B > NPK > NK over the two years (Figure 2B), with differences between all treatments reaching significant levels compared to NK ($p < 0.05$). Compared with NK, the average concentrations of SS under NPK + B, NK + B, and NPK increased by 28.55%, 18.45%, and 14.36%, respectively, at the heading stage, and by 11.93%, 20.67%, and 30.14%, respectively, at the filling stage (Figure 2C). Additionally, the differences between NPK + B and the other treatments (NK, NPK, and NK + B) were significant ($p < 0.05$). The results of the two-way ANOVA indicated no significant interaction effects of biochar (T) and year (Y) on Pro, SP, and SS concentrations.

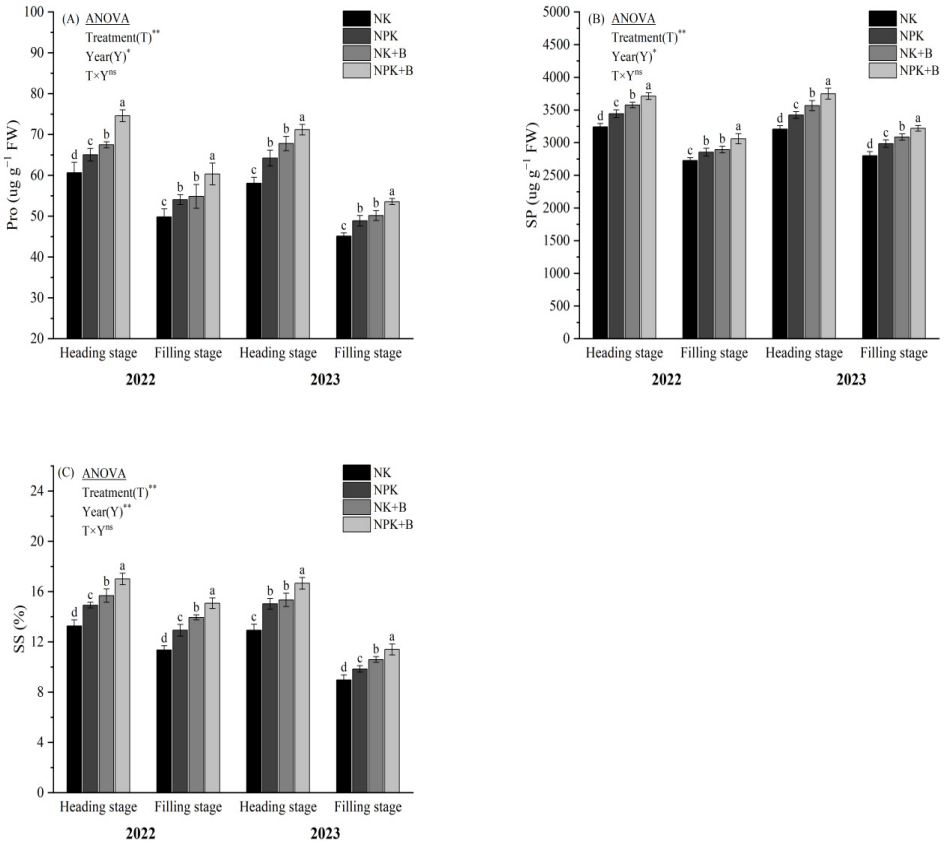

Figure 2. Effect of biochar combined with phosphorus on the proline (Pro) (**A**), soluble protein (SP) (**B**), and soluble sugar (SS) (**C**) concentration of rice leaves in two periods. NK (225 kg N, 75 kg K ha^{-1} year^{-1}), NPK (225 kg N, 70 kg P, 75 kg K ha^{-1} year^{-1}), NK + B [225 kg N, 75 kg K ha^{-1} year^{-1}, 1.5% biochar (w/w)], and NPK + B [225 kg N, 70 kg P, 75 kg K ha^{-1} year^{-1}, 1.5% biochar (w/w)]. Note: ns, not significant; * and **, significant at $p < 0.05$ and $p < 0.01$. Different letters indicate significantly different values ($p < 0.05$).

3.3. Leaf MDA, O_2^-, and H_2O_2 Concentration

As shown in Figure 3, the concentrations of MDA, O_2^-, and H_2O_2 significantly decreased after the application of biochar ($p < 0.05$). Compared to NK, the average concentrations of MDA under NPK + B, NK + B, and NPK at the heading stage were reduced by 26.39%, 19.11%, and 14.38%, respectively, and by 23.89%, 18.42%, and 10.31% at the filling stage (Figure 3A). A significant difference was observed between NPK + B and the no biochar treatments (NK and NPK) at both growth stages ($p < 0.05$). The O_2^- concentration displayed a trend of NK > NPK > NK + B > NPK + B at both growth stages over the two experimental years (Figure 3B). The differences between NPK + B and the other treatments (NK, NPK, and NK + B) were significant ($p < 0.05$). For H_2O_2, the average concentrations under NPK + B, NK + B, and NPK decreased by 25.11%, 17.79%, and 8.94% compared to NK at the heading stage, and by 20.45%, 13.52%, and 5.89% at the filling stage, respectively (Figure 3C). A significant difference was observed among all treatments ($p < 0.05$).

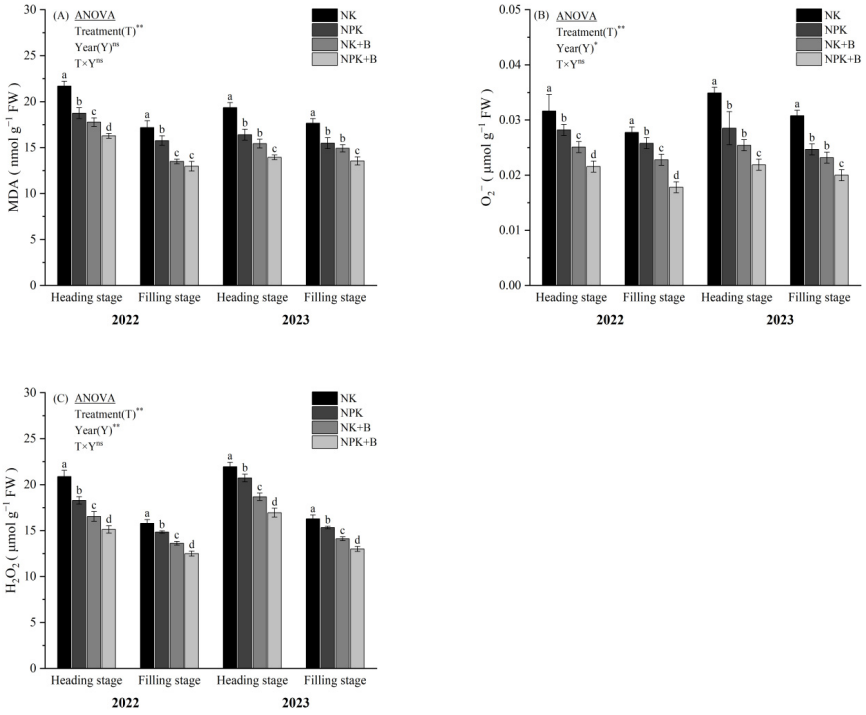

Figure 3. Effect of biochar combined with phosphorus on the Malondialdehyde (MDA) (**A**), superoxide anion(O_2^-) (**B**), and hydrogen peroxide (H_2O_2) (**C**) concentration of rice leaves in two periods. NK (225 kg N, 75 kg K ha^{-1} year^{-1}), NPK (225 kg N, 70 kg P, 75 kg K ha^{-1} year^{-1}), NK + B [225 kg N, 75 kg K ha^{-1} year^{-1}, 1.5% biochar (*w*/*w*)], and NPK + B [225 kg N, 70 kg P, 75 kg K ha^{-1} year^{-1}, 1.5% biochar (*w*/*w*)]. Note: ns, not significant; * and **, significant at $p < 0.05$ and $p < 0.01$. Different letters indicate significantly different values ($p < 0.05$).

3.4. Leaf SOD, POD, CAT, and APX Concentration

Biochar, especially when combined with phosphorus fertilizer, had a significant effect on the concentrations of SOD, POD, CAT, and APX (Figure 4). The SOD concentration showed a trend of NPK + B > NK + B > NPK > NK over the two experimental years (Figure 4A). The difference between all treatments reached a significant level ($p < 0.05$). Additionally, the SOD concentration in 2023 was significantly lower than that in 2022. Compared with NK, the average POD concentrations of NPK + B, NK + B, and NPK at the heading stage increased by 11.18%, 7.40%, and 5.96%, respectively, and by 10.91%, 6.86%, and 4.36% at the filling stage (Figure 4B). A significant difference between NPK + B and the other treatments was observed ($p < 0.05$). Regardless of phosphorus application, biochar significantly increased the CAT concentration (Figure 4C). Compared with NK, the average concentrations of CAT under NPK + B, NK + B, and NPK increased by 19.95%, 13.37%, and 10.06%, respectively, at the heading stage, and by 26.21%, 12.42%, and 9.01% at the filling stage. The average APX concentration exhibited a trend of NPK + B > NK + B > NPK > NK at both growth stages over the two years (Figure 4D). A significant difference was observed between NPK + B and the other treatments ($p < 0.05$).

3.5. Leaf ACP Concentration

As shown in Figure 5, the combined application of biochar and phosphate fertilizer significantly increased the ACP concentration. Compared with NK, the average concentrations of ACP under NPK + B, NK + B, and NPK increased by 46.55%, 32.23%, and 11.25% at the heading stage, respectively, and by 53.29%, 37.50%, and 19.08% at the filling stage, respectively. Additionally, the difference between all treatments reached a significant level ($p < 0.05$).

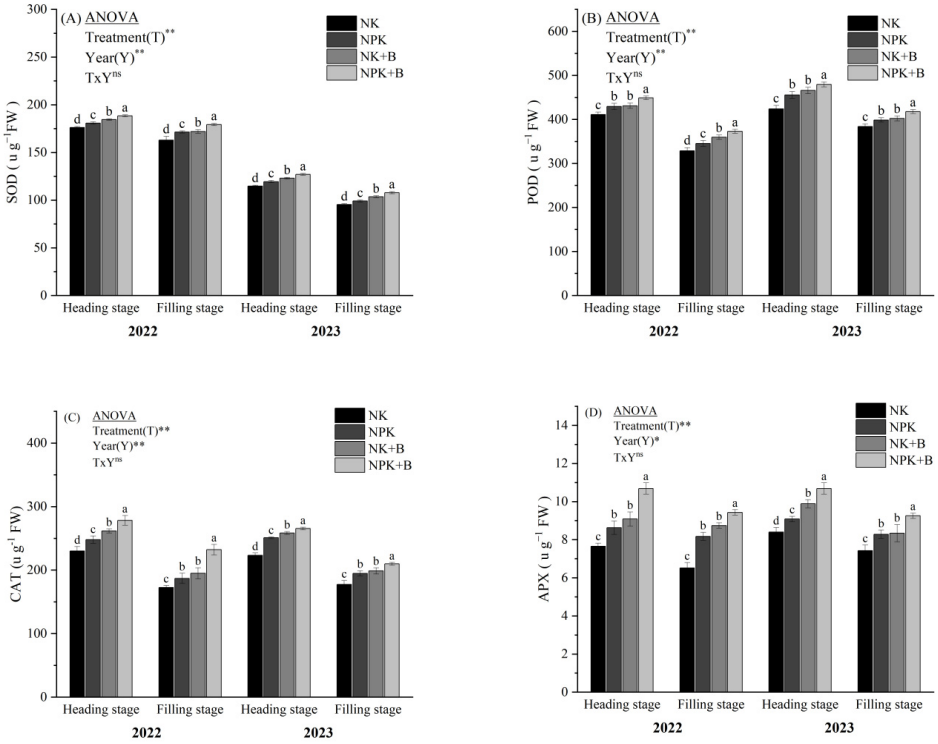

Figure 4. Effect of biochar combined with phosphorus on the superoxide dismutase (SOD) (**A**), catalase (CAT) (**B**), peroxidase (POD) (**C**), and ascorbate peroxidase (APX) (**D**) concentration of rice leaves in two periods. NK (225 kg N, 75 kg K ha^{-1} year^{-1}), NPK (225 kg N, 70 kg P, 75 kg K ha^{-1} year^{-1}), NK + B [225 kg N, 75 kg K ha^{-1} year^{-1}, 1.5% biochar (w/w)], and NPK + B [225 kg N, 70 kg P, 75 kg K ha^{-1} year^{-1}, 1.5% biochar (w/w)]. Note: ns, not significant; * and **, significant at $p < 0.05$ and $p < 0.01$. Different letters indicate significantly different values ($p < 0.05$).

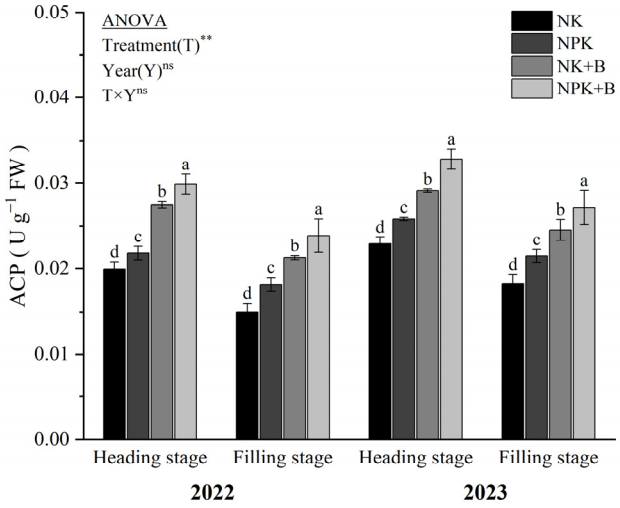

Figure 5. Effect of biochar combined with phosphorus on the acid phosphatase concentration of rice leaves in two periods. NK (225 kg N, 75 kg K ha^{-1} year^{-1}), NPK (225 kg N, 70 kg P, 75 kg K ha^{-1} year^{-1}), NK + B [225 kg N, 75 kg K ha^{-1} year^{-1}, 1.5% biochar (w/w)], and NPK + B [225 kg N, 70 kg P, 75 kg K ha^{-1} year^{-1}, 1.5% biochar (w/w)]. Note: ns, not significant; and **, significant at $p < 0.01$. Different letters indicate significantly different values ($p < 0.05$).

3.6. Plant Phosphorus Accumulation and Transport

Biochar significantly increased phosphorus accumulation in rice plants grown in soda saline-alkali land, with the highest levels observed in the NPK + B treatment across all growth stages (Table 3). Compared to the NK treatment, the average phosphorus accu-

mulation at the tillering stage increased by 67.78%, 27.73%, and 37.89% for the NPK + B, NK + B, and NPK treatments, respectively, with significant differences observed across all treatments ($p < 0.05$). The jointing stage showed the following trend: NPK + B > NK + B > NPK > NK. At the heading stage, phosphorus accumulation in the NPK + B, NK + B, and NPK treatments increased by 40.34%, 24.04%, and 25.42%, respectively, compared to the NK, with significant differences observed between the NPK + B treatment and the others ($p < 0.05$). The filling stage exhibited the following trend: NPK + B > NK + B > NPK > NK, with significant differences observed among all treatments ($p < 0.05$). Compared to the NK treatment, the average phosphorus accumulation at the maturity stage increased by 27.37%, 11.41%, and 13.68% for the NPK + B, NK + B, and NPK treatments, respectively, with significant differences observed across all treatments ($p < 0.05$). In 2023, phosphorus accumulation in plants decreased during the tillering and filling stages compared to 2022, while it increased during the jointing, heading, and maturity stages. A significant difference was observed between the NPK + B treatment and the other treatments in both years ($p < 0.05$). Two-way ANOVA analysis indicated a significant effect of treatments (T) and years (Y) on phosphorus accumulation, with no significant interaction between treatments and years.

Table 3. Phosphorus accumulation in five stages of rice in 2022 and 2023.

Year	Treatment	Tillering Stage (kg ha^{-1})	Jointing Stage (kg ha^{-1})	Heading Stage (kg ha^{-1})	Filling Stage (kg ha^{-1})	Maturity Stage (kg ha^{-1})
2022	NK	4.53 ± 0.07 d	10.92 ± 0.50 d	13.74 ± 0.12 c	23.78 ± 0.35 d	31.22 ± 0.47 d
	NPK	6.13 ± 0.06 b	15.36 ± 0.27 b	17.32 ± 0.12 b	28.79 ± 0.54 c	35.53 ± 0.48 b
	NK + B	5.70 ± 0.04 c	14.38 ± 0.31 c	17.14 ± 0.23 b	29.74 ± 0.64 b	34.81 ± 0.26 c
	NPK + B	7.41 ± 0.06 a	15.81 ± 0.54 a	19.43 ± 0.21 a	33.07 ± 0.36 a	37.94 ± 0.19 a
2023	NK	3.37 ± 0.05 d	12.75 ± 0.51 c	14.76 ± 0.11 c	23.59 ± 0.36 d	32.66 ± 0.47 d
	NPK	4.77 ± 0.06 b	15.23 ± 0.71 b	18.42 ± 0.12 b	28.54 ± 0.54 c	37.10 ± 0.48 b
	NK + B	4.39 ± 0.04 c	14.79 ± 0.34 b	18.21 ± 0.22 b	29.47 ± 0.62 b	36.37 ± 0.27 c
	NPK + B	5.84 ± 0.06 a	16.63 ± 0.23 a	20.57 ± 0.20 a	32.76 ± 0.35 a	39.60 ± 0.20 a
Source of variation						
Treatment (T)		*	*	**	**	**
Year (Y)		*	*	*	**	**
T × Y		ns	ns	ns	ns	ns

Different means followed by different letters indicate that the values differ at the level of $p < 0.05$. Note: ns, not significant; * and **, significant at $p < 0.05$ and $p < 0.01$, respectively Values are means ± SD.

The results presented in Table 4 indicate a significant increase in stem-sheath phosphorus transport, leaf phosphorus transport, phosphorus transport efficiency, and panicle phosphorus content in rice grown in soda saline-alkali soil after the application of biochar. The average phosphorus transportation amount and efficiency in the stem-sheath followed the trend: NPK + B > NK + B > NPK > NK. A significant difference was observed between NPK + B and the other treatments ($p < 0.05$). In 2023, there was a notable increase in both the volume and efficiency of phosphorus transport in the stem-sheath compared to 2022. Additionally, the two-year findings for leaf phosphorus transport and efficiency mirrored those observed for stem-sheath phosphorus transport. Compared to the NK treatment, the average increases in phosphorus content in the panicles for the NPK + B, NK + B, and NPK treatments were 20.43%, 10.66%, and 12.56%, respectively. Significant differences were observed between the NPK + B treatment and the other treatments ($p < 0.05$). Two-way ANOVA analysis indicated significant effects on phosphorus transport and transport efficiency in the stem sheath and leaf across different treatments and years.

Table 4. Phosphorus transport volume and phosphorus transport efficiency of rice in 2022 and 2023.

Year	Treatment	P Transportation Amount in Stem-Sheath (kg ha^{-1})	P Transportation of Stem-Sheath Efficiency (%)	P Transportation Amount in Leaf (kg ha^{-1})	P Transportation of Leaf Efficiency (%)	P Increment Amount in Panicle (kg ha^{-1})
2022	NK	1.64 ± 0.06 c	25.67 ± 1.04 c	1.30 ± 0.05 c	55.38 ± 1.14 c	20.42 ± 0.63 c
	NPK	2.72 ± 0.03 b	34.02 ± 0.31 b	2.07 ± 0.03 b	63.42 ± 0.89 b	23.00 ± 0.55 b
	NK + B	2.79 ± 0.07 b	35.05 ± 0.43 b	2.14 ± 0.01 b	63.16 ± 0.64 b	22.60 ± 0.33 b
	NPK + B	3.32 ± 0.08 a	37.45 ± 0.60 a	2.78 ± 0.06 a	68.59 ± 0.99 a	24.61 ± 0.26 a
2023	NK	1.85 ± 0.06 c	26.11 ± 0.92 c	1.37 ± 0.05 c	55.09 ± 1.02 c	21.13 ± 0.63 c
	NPK	2.94 ± 0.03 b	33.75 ± 0.25 b	2.15 ± 0.03 b	62.93 ± 0.86 b	23.77 ± 0.55 b
	NK + B	3.00 ± 0.07 b	34.65 ± 0.41 b	2.22 ± 0.01 b	62.83 ± 0.54 b	23.38 ± 0.33 b
	NPK + B	3.55 ± 0.07 a	36.90 ± 0.54 a	2.85 ± 0.06 a	67.93 ± 0.93 a	25.43 ± 0.26 a
Source of variation						
Treatment (T)		**	**	**	**	*
Year (Y)		**	**	**	**	*
T × Y		ns	ns	ns	ns	ns

Different means followed by different letters indicate that the values differ at the level of $p < 0.05$. Note: ns, not significant; * and **, significant at $p < 0.05$ and $p < 0.01$, respectively. Values are means ± SD.

3.7. Phosphorus Use Efficiency

The analysis of variance indicated that biochar significantly affected several phosphorus-related parameters in rice grown in soda saline-alkali fields, including the phosphorus harvest index, phosphate use efficiency, phosphorus uptake efficiency, partial productivity of phosphorus fertilizer, and phosphate agronomic use efficiency (Table 5). The combination of biochar and phosphorus fertilizer (NPK + B) enhanced the phosphorus harvest index in soda saline rice fields more effectively than biochar alone, though this difference was only significant in 2022 ($p < 0.05$). Additionally, the phosphorus harvest index rose in 2023 compared to 2022. Compared to the NPK treatment, phosphorus utilization efficiency in the NPK + B treatment increased by 56.56% in 2022 and 55.68% in 2023. In both 2022 and 2023, phosphorus absorption efficiency, phosphorus fertilizer partial productivity, and agronomic utilization of phosphorus fertilizer all demonstrated a trend of NPK + B being greater than NPK. A significant difference was observed between NPK + B and NPK treatments ($p < 0.05$).

Table 5. Phosphorus use efficiency in rice in 2022 and 2023.

Year	Treatment	Phosphorus Harvest Index (%)	Phosphorus Fertilizer Use Efficiency (%)	Phosphorus Absorption Efficiency (%)	PFP (kg kg)	PAE (kg kg)
2022	NK	80.55 ± 0.58 b				
	NPK	81.03 ± 0.19 ab	6.33 ± 1.31 b	52.99 ± 0.69 b	102.44 ± 1.55 b	14.58 ± 0.95 b
	NK + B	80.82 ± 0.33 ab				
	NPK + B	81.27 ± 0.14 a	9.91 ± 0.93 a	56.57 ± 0.29 a	120.60 ± 3.07 a	32.74 ± 2.18 a
2023	NK	81.41 ± 0.61 a				
	NPK	81.76 ± 0.19 a	6.16 ± 1.30 b	50.76 ± 0.69 b	116.57 ± 1.66 b	15.81 ± 0.96 b
	NK + B	81.56 ± 0.34 a				
	NPK + B	82.02 ± 0.15 a	9.59 ± 0.90 a	54.19 ± 0.27 a	136.09 ± 3.28 a	35.32 ± 2.39 a
Source of variation						
Treatment (T)		ns	*	*	*	ns
Year (Y)		ns	ns	ns	ns	ns
T × Y		ns	ns	ns	ns	ns

Different means followed by different letters indicate that the values differ at the level of $p < 0.05$. Note: ns, not significant; *, significant at $p < 0.05$, respectively. Values are means ± SD.

3.8. Rice Biomass Yield, Grain Yield, and Harvest Index

The biomass yield, grain yield, and harvest index of rice in soda saline-alkali soil were significantly increased under the combined application of biochar and phosphate fertilizer (Table 6). Compared with NK, the biomass yield for NPK + B, NK + B, and NPK increased by 12.29%, 6.32%, and 6.60%, respectively, on average, with significant differences observed between NPK + B and other treatments in both years ($p < 0.05$). For grain yield, NPK + B, NK + B, and NPK increased by 41.91%, 23.01%, and 20.05% compared to NK in 2022, and by 42.34%, 22.55%, and 19.57% in 2023, respectively. The harvest index exhibited the trend NPK + B > NK + B > NPK > NK over the two-year period, with a significant difference between NPK + B and the other treatments ($p < 0.05$). Moreover, the rice harvest index improved with each subsequent year of field re-entry. A two-way ANOVA revealed significant interaction effects between biochar application and years on biomass yield, grain yield, and harvest index.

Table 6. Rice yield and biomass in 2022 and 2023.

Year	Treatment	Biomass Yield (t ha^{-1})	Grain Yield (t ha^{-1})	Harvested Index
2022	NK	13.16 ± 0.07 c	4.39 ± 0.09 c	0.33 ± 0.01 c
	NPK	13.92 ± 0.04 b	5.27 ± 0.08 b	0.37 ± 0.00 b
	NK + B	13.92 ± 0.07 b	5.40 ± 0.08 b	0.38 ± 0.01 b
	NPK + B	14.67 ± 0.11 a	6.23 ± 0.10 a	0.41 ± 0.01 a
2023	NK	13.13 ± 0.07 c	4.70 ± 0.09 c	0.36 ± 0.01 c
	NPK	14.09 ± 0.04 b	5.62 ± 0.09 b	0.40 ± 0.01 b
	NK + B	14.02 ± 0.06 b	5.76 ± 0.10 b	0.41 ± 0.01 b
	NPK + B	14.84 ± 0.11 a	6.69 ± 0.10 a	0.45 ± 0.01 a
Source of variation				
Treatment (T)		**	**	*
Year (Y)		*	**	*
T × Y		*	*	*

Different means followed by different letters indicate that the values differ at the level of $p < 0.05$. Note: * and **, significant at $p < 0.05$ and $p < 0.01$, respectively. Values are means ± SD.

3.9. Correlation and Principal Component Analysis of Sodium and Potassium Ions, Physiological Indexes, Phosphorus Use Efficiency, and Yield

The relationship between rice yield and sodium-potassium ions, physiological indices, and phosphorus use efficiency is illustrated in Figure 6. The results indicate that grain yield had a significant positive correlation with phosphorus use efficiency, plant phosphorus accumulation (PA), superoxide dismutase (SOD), catalase (CAT), peroxidase (POD), ascorbate peroxidase (APX), soluble protein (SP), soluble sugars (SS), proline (Pro), acid phosphatase (ACP), and potassium ion concentration (K^+) ($p < 0.01$). Conversely, grain yield was negatively correlated with malondialdehyde (MDA), superoxide anion (O_2^-), hydrogen peroxide (H_2O_2), sodium ion concentration (Na^+), and the Na^+/K^+ ratio ($p < 0.01$). Additionally, phosphorus use efficiency (PUE) showed positive correlations with PA, SOD, CAT, POD, APX, SP, SS, Pro, and ACP, and negative correlations with MDA, O_2^-, H_2O_2, and Na^+ ($p < 0.05$). Plant phosphorus accumulation (PA) exhibited significant positive correlations with SOD, CAT, POD, APX, SP, SS, Pro, and ACP ($p < 0.01$), while showing negative correlations with MDA, O_2^-, H_2O_2, and Na^+ ($p < 0.01$).

In the principal component analysis (Figure 7), PC1 accounted for 89.5% of the total variation in crop yield and antioxidant enzymes, osmotic regulators, and acid phosphatase, showing a significant positive correlation. PC2 explained 4.4% of the variation based on reactive oxygen species, malondialdehyde, and sodium ions, displaying a significant negative correlation.

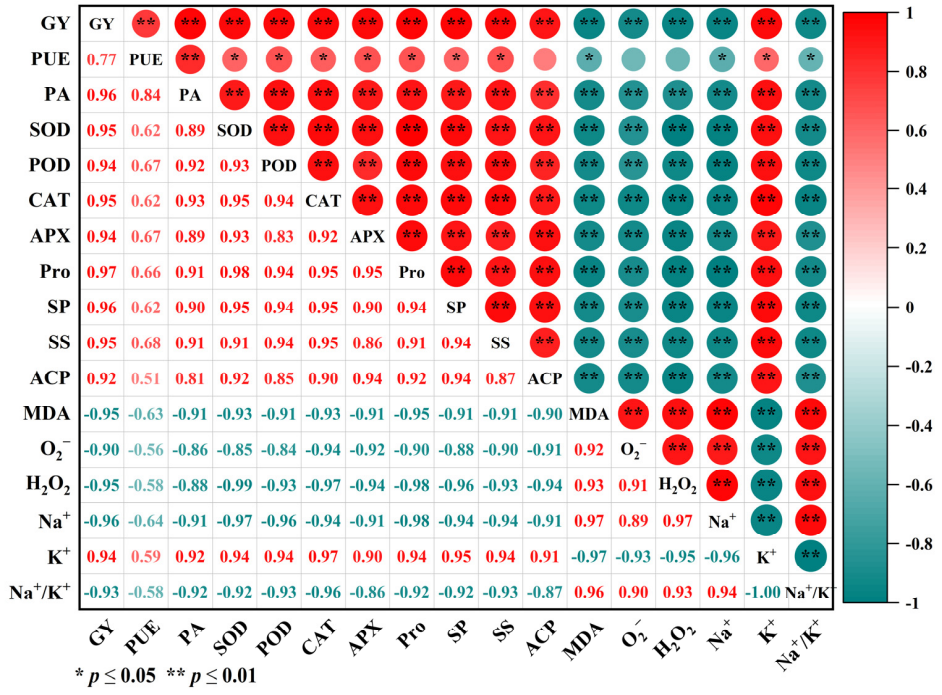

Figure 6. The correlations (R^2) of superoxide dismutase (SOD), catalase (CAT), peroxidase (POD), ascorbate peroxidase (APX), Malondialdehyde (MDA), superoxide anion(O_2^-), hydrogen peroxide (H_2O_2), proline (Pro), soluble protein (SP), soluble sugar (SS), acid phosphatase (ACP), Na^+, K^+, Na^+/K^+, phosphorus use efficiency (PUE), phosphorus accumulation (PA), and grain yield (GY) under biochar and phosphorus combinations. Different letters indicate significantly different values ($p < 0.05$); *, and **, significant at $p < 0.05$, and $p < 0.01$ level, respectively. Error bars indicated standard error of the mean.

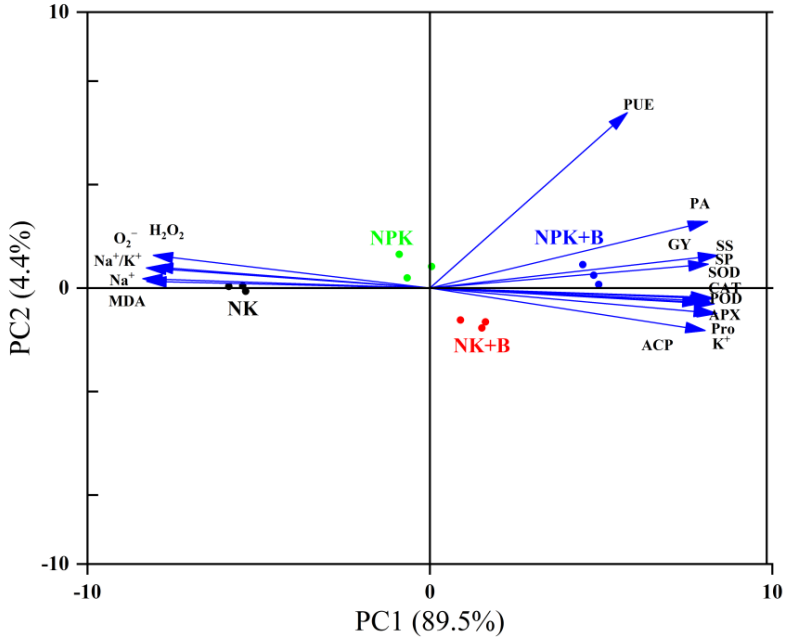

Figure 7. The principal component analysis (PCA) of superoxide dismutase (SOD), catalase (CAT), peroxidase (POD), ascorbate peroxidase (APX), malondialdehyde (MDA), superoxide anion(O_2^-), hydrogen peroxide H_2O_2, proline (Pro), soluble protein (SP), soluble sugar (SS), acid phosphatase (ACP), Na^+, K^+, Na^+/K^+, phosphorus use efficiency (PUE), phosphorus accumulation (PA), and grain yield (GY) under biochar and phosphorus combinations. Each point for each treatment represents three replicates. Error bars indicated standard error of the mean.

4. Discussion

4.1. Effects of the Combined Application of Biochar and Phosphate Fertilizer on Ionic Accumulation in Rice Organs in Soda Saline-Alkali Land

The high concentration of Na^+ ions not only hinders the uptake of K^+ ions by the root system but also disrupts various physiological and biochemical processes in crop cells, thereby restricting the normal growth and development of crops [30,46]. Previous studies have shown that increasing K^+ concentrations in plant tissues can alleviate salt stress and promote plant growth [29,34]. Numerous studies have demonstrated that incorporating biochar into soil can lower soil bulk density, enhance soil organic carbon and cation exchange capacity, and improve soil structure [47]. The porous structure and extensive surface area of biochar can effectively reduce the influx of Na^+ into crop cells, thereby mitigating crop damage caused by salt stress [30,36,48]. Song et al. [49] discovered that increasing K^+ concentration and the K^+/Na^+ ratio effectively enhanced peanut growth and yield in saline soil. In this study, we found that incorporating biochar into soda saline-alkali paddy soils led to a significant decrease in Na^+ concentration (Figure 1A) and Na^+/K^+ ratio (Figure 1C) in rice organs, while also increasing K^+ concentration (Figure 1B). Results from the present study demonstrated the potential of biochar to alleviate Na^+ toxicity in highly saline-alkali paddy fields. This may be due to several reasons: (i) biochar has a high Na^+ adsorption capacity, effectively removing Na^+ from the soil solution [29]; (ii) biochar serves as a direct source of minerals such as Ca^{2+} and Mg^{2+}, which play a crucial role in replacing Na^+ at the exchange sites [50]; (iii) the enhancement in Na^+ adsorption and K^+ uptake contributes to achieving ionic balance in plant organs (Figure 1) and helps mitigate oxidative stress (Figure 3). The combined application of biochar and phosphate fertilizer was more effective in increasing K^+ concentration than using phosphate fertilizer alone (Figure 1B). This is likely due to the application of phosphorus in salt-affected soils with poor fertility, which promotes the selective transport of K^+, Ca^{2+}, and Mg^{2+}, improves the ionic balance in various organs, and alleviates ionic competition caused by salt [51]. This is a key factor contributing to the superior performance of the combined application compared to using phosphate fertilizer alone.

4.2. Effect of Combined Application of Biochar and Phosphate Fertilizer on Physiological Indexes of Rice in Soda Saline-Alkali Land

The concentration of salt in saline-alkali soils exceeds the levels necessary for optimal plant growth, resulting in osmotic stress. Additionally, ionic toxicity damages plant cell membranes, leading to the accumulation of reactive oxygen species (ROS) in plant organelles, which hinders plant growth and development [52,53]. To maintain ROS balance and inhibit the production of malondialdehyde (MDA), plants produce antioxidant enzymes to mitigate saline-alkali stress [54]. They also counteract this stress by synthesizing proline, soluble sugars, and other organic osmolytes that support growth [55]. The increase in acid phosphatase (ACP) activity is widely recognized as a critical adaptation for plants in low-phosphorus environments, enhancing their ability to absorb and utilize phosphorus [56]. He et al. [57] demonstrated that incorporating 2.0% and 2.5% biochar significantly decreased malondialdehyde (MDA) levels while increasing proline (Pro) and water-soluble sugar (WSS) content in *Miscanthus vulgaris*. Previous studies have shown that biochar modulates antioxidant enzyme levels in plants, alleviating salt stress and reducing free radical accumulation [31,58]. This regulation can help alleviate salt stress and ultimately enhance plant growth. The study found a significant increase in the levels of proline (Pro), soluble proteins (SP), and soluble sugars (SS) in rice grown in soda saline-alkali soil following the application of biochar (Figure 2). This finding aligns with the research of Zhang et al. [59], who reported that biochar application increased soluble sugars and proline levels in maize, thereby enhancing osmotic regulation and stress resistance. In contrast, Obadi et al. [60] observed different results, noting that under specific conditions, such as salt stress and water deficit, biochar could actually decrease proline content in plants. It is speculated that the loose, porous structure of biochar improves soil quality,

reduces osmotic pressure, and facilitates the uptake of water and nutrients. We found that the application of biochar significantly increased the levels of antioxidant enzymes and reduced the accumulation of MDA and ROS in the leaves of rice grown in saline-alkaline soil (Figures 3 and 4). This effect may be attributed to biochar's ability to alleviate oxidative stress in plants by activating antioxidant enzymes [61]. Additionally, we observed that the application of biochar increased the acid phosphatase content in rice leaves grown in soda saline-alkali soil (Figure 2). This increase may be due to the nutrient-rich nature of biochar, which enhances microbial activity and subsequently boosts phosphatase activity [28]. The results demonstrated that biochar has the potential to enhance the levels of antioxidant enzymes, osmotic regulators, and acid phosphatase, leading to reduced ROS production, improved plant resistance, and mitigation of saline-alkali stress. These outcomes may be attributed to the following factors: (i) biochar improves the physical and chemical properties of saline-alkali soil, alleviating oxidative and osmotic stress in plants under saline-alkali conditions [34]; (ii) the application of biochar significantly decreased the levels of Na^+ and the Na^+/K^+ ratio in soda saline-alkali soil, leading to reduced ionic toxicity (Figure 1).

The study also revealed that the combined application of biochar and phosphate fertilizer significantly increased the concentrations of antioxidant enzymes, osmotic regulators, and acid phosphatase in rice while reducing the levels of ROS and MDA (Figures 2–5). This effect may be due to the increased phosphorus fertilization significantly improving antioxidant enzyme activity and alleviating the physiological mechanisms of salt stress in crops [62]. Correlation analysis revealed that antioxidant enzymes were positively correlated with osmotic regulators and K^+, while showing negative correlations with ROS, MDA, Na^+, and Na^+/K^+ ratios.

4.3. Relationship between Biochar and Phosphate Fertilizer and Phosphorus Accumulation and Utilization Efficiency of Rice in Soda Saline-Alkali Land

Salt stress diminishes the external water potential of plant roots, resulting in osmotic stress and ionic toxicity from sodium or chloride ions. This disruption affects the absorption and transport of phosphorus [12]. Elevated salt levels create competition between salt ions and phosphate, ultimately reducing the activity of phosphorus transporters and decreasing phosphorus uptake efficiency [63]. Biochar has been shown to enhance the nutrient content of saline-alkali soil, improve soil aggregate stability, reduce nutrient leaching, increase phosphatase activity and the populations of rhizosphere microorganisms, facilitate organophosphorus mineralization, enhance phosphorus utilization efficiency, alleviate crop salt stress, and promote overall crop growth [64]. Strelko et al. [24] found that biochar can serve as a direct source of phosphorus, significantly increasing the availability of phosphorus in coastal saline-alkali soils. In this study, we observed that biochar significantly enhanced phosphorus accumulation, uptake, and utilization efficiency in rice plants grown in soda saline-alkali soil (Tables 3–5). This improvement may be attributed to several factors. Firstly, the presence of acidic groups such as hydroxyl, carboxyl, and nitro on biochar's surface can lower soil pH, prevent the formation of insoluble complexes between phosphate and soil cations, and enhance soil phosphorus efficiency [65]. Secondly, studies have shown that the addition of biochar can provide a nitrogen source for plants, improve the environment for phosphorus-solubilizing microorganisms, and promote phosphorus absorption by plants [66]. Lastly, biochar decreases ionic toxicity, mitigates salinity stress, and promotes phosphorus uptake (Figures 1–3). This study revealed that the combination of biochar and phosphorus fertilizer significantly increased phosphorus utilization efficiency and uptake in soda saline-alkali soil (Table 5). Consistent with previous research, Elgharably et al. [67] found that applying phosphorus under NaCl stress led to an increase in phosphorus content in wheat stems, as well as enhanced phosphorus uptake and utilization. This effect may be attributed to the competition between phosphate groups and salt ions, which mitigates the impact of salt stress [51]. Correlation analysis showed a significant positive relationship between phosphorus absorption and utilization efficiency

with antioxidant enzymes, osmotic regulators, and K^+ ($p < 0.05$). Conversely, a negative correlation was observed with malondialdehyde, Na^+, and Na^+/K^+ ratios ($p < 0.05$).

4.4. Relationship between Biochar and Phosphate Fertilizer and Rice Yield in Soda Saline-Alkali Land

Crops in saline land encounter several challenges that impede growth and yield, including: (i) the accumulation of reactive oxygen species (ROS), which reduces leaf photosynthetic rates [68]; (ii) metabolic disorders from elevated Na^+ concentrations [4]; (iii) high osmotic pressure in the soil solution, resulting in decreased water availability for crops [35]; (iv) restricted absorption of essential nutrients due to high Na^+ levels [29]; (v) inhibited root growth caused by poor soil structure [9]. Research has shown that applying biochar can enhance crop growth and yields in saline-alkali soil by improving plant physiological functions, increasing tolerance to saline-alkali stress, and promoting overall growth under these conditions [35,36,69].

Our previous research has demonstrated that biochar can enhance the physical and chemical properties of soda saline-alkali soil, increase soil organic carbon content, and enrich mineral nutrients. Additionally, the porous nature of biochar can boost microbial community diversity and soil enzyme activities, improve plant salt tolerance, and stimulate plant growth in saline-alkali soil [32–35]. Applying phosphate fertilizer can improve the growth of rice stems and roots under stressful conditions, such as in saline-alkali soil, leading to an increased number of panicles per unit area, a higher seed-setting rate, and ultimately a boost in rice yield [70]. However, Xu et al. [71] discovered an antagonistic effect when biochar was combined with phosphorus fertilizer in saline-alkali soil. The addition of biochar can enhance the adsorption or precipitation of phosphorus, reducing its availability and ultimately leading to decreased crop biomass and lower phosphorus content in plants. In this study, biochar significantly influenced the biomass yield, grain yield, and harvest index of rice grown in highly soda saline-alkali soil (Table 6). The correlation analysis revealed significant positive relationships between rice yield and phosphorus use efficiency, protective enzymes, osmotic regulators, acid phosphatase, and K^+ ($p < 0.01$), while negative correlations were observed with reactive oxygen species, malondialdehyde, and sodium ions ($p < 0.01$). Our results indicated that the synergistic application of biochar and phosphorus fertilizer significantly improved ionic balance, increased antioxidant enzyme activity, reduced oxidative damage, enhanced phosphorus use efficiency, and ultimately led to a higher rice yield ($p < 0.05$). These outcomes may be attributed to several factors. First, biochar acts as an adsorbent, sequestering Na^+ ions while simultaneously releasing mineral nutrients into the soil solution. This mechanism leads to a significant reduction in Na^+ concentration (Figure 1A) and the Na^+/K^+ ratio (Figure 1C) in rice organs grown in soda saline-alkali soil, while also increasing K^+ concentration (Figure 1B) [72]. Second, biochar significantly enhances osmoregulatory substances and antioxidant enzymes (Figures 2 and 4), reduces levels of reactive oxygen species and malondialdehyde (Figure 3), and improves the physiological condition of rice cultivated in soda saline soil. Lastly, biochar can improve phosphorus uptake by crops and enhance the efficiency of phosphorus fertilizers in the soil, resulting in increased grain yield (Tables 3–5). Mahmoud et al. [73] found that the combined application of phosphate fertilizer and biochar increased both wheat yield and soil phosphorus content in alkaline soils. In line with previous research, our study's results also demonstrate that the mixed use of biochar and phosphorus fertilizer significantly boosted biomass yield, grain yield, and harvest index in rice grown in severely soda saline-alkali soil (Table 6). These enhancements can be attributed to improvements in soil physicochemical properties, increased phosphorus availability, reduced nutrient leaching, and enhanced plant uptake and utilization of phosphorus due to the integrated application of biochar, straw, and phosphorus fertilizer [74,75].

5. Conclusions

A two-year field experiment demonstrated that the combined application of biochar and phosphate fertilizer (NPK + B) significantly alleviated ion toxicity, osmotic stress, and oxidative damage in rice cultivated in soda saline-alkali paddy fields ($p < 0.05$). This was achieved by significantly reducing Na^+ concentration and the Na^+/K^+ ratio in rice organs while enhancing K^+ concentration, antioxidant enzyme levels, and osmotic stress tolerance. Correlation and principal component analyses showed that indicators such as protective enzymes and osmoregulatory substances were significantly positively correlated with yield and phosphorus utilization efficiency but significantly negatively correlated with ROS. Consequently, phosphorus absorption and utilization were improved, ultimately resulting in higher rice yields. These findings offer new insights into the use of biochar to enhance phosphorus use efficiency and yield in soda saline-alkali paddy fields. However, further research is needed to investigate the environmental and economic benefits of combining biochar with fertilizers.

Author Contributions: Conceptualization, F.J.; writing—review and editing, X.L.; software, W.C. and J.P.; formal analysis, Y.S., X.W. and Y.Z.; data curation S.M. and H.W.; investigation, L.X. and J.S. All authors have read and agreed to the published version of the manuscript.

Funding: This study was funded by the National Natural Science Foundation of China (No. 32071951), and Natural Science Foundation of Jilin Province (No. 20230101258JC).

Institutional Review Board Statement: Not applicable.

Informed Consent Statement: Not applicable.

Data Availability Statement: The data that support the findings of this study are available from the corresponding author upon reasonable request.

Conflicts of Interest: The authors declare no conflict of interest.

References

1. Gong, H.Y.; Li, Y.F.; Li, S.J. Effects of the interaction between biochar and nutrients on soil organic carbon sequestration in soda saline-alkali grassland: A review. *Glob. Ecol. Conserv.* **2021**, *26*, e01449. [CrossRef]
2. Yang, Y.Q.; Guo, Y. Elucidating the molecular mechanisms mediating plant salt-stress responses. *New Phytol.* **2018**, *217*, 523–539. [CrossRef] [PubMed]
3. Kamran, M.; Xie, K.; Sun, J.; Wang, D.; Shi, C.H.; Lu, Y.S.; Gu, W.J.; Xu, P.Z. Modulation of growth performance and coordinated induction of ascorbate-glutathione and methylglyoxal detoxification systems by salicylic acid mitigates salt toxicity in choysum (*Brassica parachinensis* L.). *Ecotoxicol. Environ. Saf.* **2020**, *188*, 109877. [CrossRef] [PubMed]
4. Ling, F.L.; Su, Q.W.; Jiang, H.; Cui, J.J.; He, X.L.; Wu, Z.H.; Zhang, Z.A.; Liu, J.; Zhao, Y.J. Effects of strigolactone on photosynthetic and physiological characteristics in salt-stressed rice seedlings. *Sci. Rep.* **2020**, *10*, 6183. [CrossRef]
5. Wong, V.N.L.; Greene, R.S.B.; Dalal, R.C.; Murphy, B.W. Soil carbon dynamics in saline and sodic soils: A review. *Soil Use Manag.* **2010**, *26*, 2–11. [CrossRef]
6. Santos, W.M.; Gonzaga, M.I.S.; Silva, J.A.; Almeida, A.Q.; Santos, J.C.J.; Gonzaga, T.A.S.; Lima, I.S.; Araújo, E.M. Effectiveness of different biochars in remediating a salt affected Luvisol in Northeast Brazil. *Biochar* **2021**, *3*, 149–159. [CrossRef]
7. Choudhury, F.K.; Rivero, R.M.; Blumwald, E.; Mittler, R. Reactive oxygen species, abiotic stress and stress combination. *Plant J.* **2016**, *90*, 856–867. [CrossRef]
8. Munns, R.; Tester, M. Mechanisms of Salinity Tolerance. *Annu. Rev. Plant Biol.* **2008**, *59*, 651–681. [CrossRef]
9. Guan, B.; Zhou, D.; Zhang, H.; Tian, Y.; Japhet, W.; Wang, P. Germination responses of Medicago ruthenica seeds to salinity, alkalinity, and temperature. *J. Arid. Environ.* **2009**, *73*, 135–138. [CrossRef]
10. Camenzind, T.; Hättenschwiler, S.; Treseder, K.K.; Lehmann, A.; Rillig, M.C. Nutrient limitation of soil microbial processes in tropical forests. *Ecol. Monogr.* **2018**, *88*, 4–21. [CrossRef]
11. Papadopoulos, I.; Rendig, V.V. Interactive effects of salinity and nitrogen on growth and yield of tomato plants. *Plant Soil* **1983**, *73*, 47–57. [CrossRef]
12. Long, R.C.; Sun, H.; Cao, C.Y.; Zhang, T.J.; Kang, J.M.; Wang, Z.; Li, M.N.; Gao, Y.L.; Li, X.; Yang, Q.C. Identification of alkali-responsive proteins from early seedling stage of two contrasting Medicago species by iTRAQ-based quantitative proteomic analysis. *Environ. Exp. Bot.* **2019**, *157*, 26–34. [CrossRef]
13. Wang, J.L.; Shuman, L.M. Transformation of phosphate in rice (*Oryza sativa* L.) rhizosphere and its influence on phosphorus-nutrition of rice. *J. Plant Nutr.* **1994**, *17*, 1803–1815. [CrossRef]

14. Ullah, S.; Dahlawi, S.; Naeem, A.; Rengel, Z.; Naidu, R. Biochar application for the remediation of salt-affected soils: Challenges and opportunities. *Sci. Total Environ.* **2017**, *625*, 320. [CrossRef]
15. Wan, W.J.; Qin, Y.; Wu, H.Q.; Zuo, W.L.; He, H.M.; Tan, J.D.; Wang, Y.; He, D.L. Isolation and characterization of phosphorus solubilizing bacteria with multiple phosphorus sources utilizing capability and their potential for lead immobilization in soil. *Front. Microbiol.* **2020**, *11*, 752. [CrossRef]
16. Gao, M.H.; Li, N.; Peng, J.; Chen, K.; Gao, T.Y.; Han, X.R. Effects of straw and biochar returning on soil aggregates distribution and organic carbon content in brown soil. *J. Plant Nutr. Fertil.* **2020**, *26*, 1978–1986. [CrossRef]
17. Nublat, A.; Desplans, J.; Casse, F.; Berthomieu, P. sas1, an Arabidopsis mutant overaccumulating sodium in the shoot, shows deficiency in the control of the root radial transport of sodium. *Plant Cell* **2001**, *13*, 125–137. [CrossRef]
18. Fageria, N.K.; Gheyi, H.R.; Moreira, A. Nutrient bioavailability in salt affected soils. *J. Plant Nutr.* **2011**, *34*, 945–962. [CrossRef]
19. Tian, Z.J.; Li, J.P.; Jia, X.Y.; Yang, F.; Wang, Z.C. Assimilation and Translocation of Dry Matter and Phosphorus in Rice Genotypes Affected by Salt-Alkaline Stress. *Sustainability* **2016**, *8*, 568. [CrossRef]
20. Liu, X.Y.; Yang, J.S.; Tao, J.Y.; Yao, R.J. Integrated application of inorganic fertilizer with fulvic acid for improving soil nutrient supply and nutrient use efficiency of winter wheat in a salt-affected soil. *Appl. Soil Ecol.* **2022**, *170*, 104255. [CrossRef]
21. Li, H.B.; Dong, X.L.; Da Silva, E.B.; De Oliveira, L.M.; Chen, Y.S.; Ma, L.Q. Mechanisms of metal sorption by biochars: Biochar characteristics and modifications. *Chemosphere* **2017**, *178*, 466–478. [CrossRef] [PubMed]
22. Yan, T.T.; Xue, J.H.; Zhou, Z.D.; Wu, Y.B. The Trends in research on the effects of biochar on soil. *Sustainability* **2020**, *12*, 7810. [CrossRef]
23. Duan, M.; Liu, G.H.; Zhou, B.B.; Chen, X.P.; Wang, Q.J.; Zhu, H.Y.; Li, Z.J. Effects of modified biochar on water and salt distribution and water-stable macro-aggregates in saline alkaline soil. *J. Soils Sediments* **2021**, *21*, 2192–2202. [CrossRef]
24. Strelko, V.J.; Malik, D.J.; Streat, M. Characterisation of the surface of oxidised carbon adsorbents. *Carbon* **2002**, *40*, 95–104. [CrossRef]
25. Chintala, R.; Schumacher, T.E.; Mcdonald, L.M.; Clay, D.E.; Malo, D.D.; Papiernik, S.K.; Clay, S.A.; Julson, J.L. Phosphorus sorption and availability from biochars and soil/biochar mixtures. *CLEAN Soil Air Water* **2014**, *42*, 626–634. [CrossRef]
26. Lashari, M.S.; Liu, Y.M.; Li, L.Q.; Pan, W.N.; Fu, J.Y.; Pan, G.X.; Zheng, J.F.; Zheng, J.W.; Zhang, X.H.; Yu, X.Y. Effects of amendment of biochar-manure compost in conjunction with pyroligneous solution on soil quality and wheat yield of a salt-stressed cropland from Central China Great Plain. *Field Crops Res.* **2013**, *144*, 113–118. [CrossRef]
27. Tang, J.W.; Zhang, S.D.; Zhang, X.T.; Chen, J.H.; He, X.Y.; Zhang, Q.Z. Effects of pyrolysis temperature on soil-plant-microbe responses to *Solidago canadensis* L.-derived biochar in coastal saline-alkali soil. *Sci. Total Environ.* **2020**, *731*, 138938. [CrossRef]
28. Liu, L.; Zhang, S.R.; Chen, M.M.; Fei, C.; Zhang, W.J.; Li, Y.Y.; Ding, X.D. Fe-modified biochar combined with mineral fertilization promotes soil organic phosphorus mineralization by shifting the diversity of phoD-harboring bacteria within soil aggregates in saline-alkaline paddy soil. *J. Soils Sediments* **2022**, *23*, 619–633. [CrossRef]
29. Chaganti, V.N.; Crohn, D.M. Evaluating the relative contribution of physiochemical and biological factors in ameliorating a saline–sodic soil amended with composts and biochar and leached with reclaimed water. *Geoderma* **2015**, *259–260*, 45–55. [CrossRef]
30. Li, X.; Yao, T.X.; Huang, X.X.; Li, X.B.; Li, P.Y.; Du, S.; Wang, W.; Miao, S.H.; Wang, D.; Jin, F.; et al. Biochar increases rice yield by improving root morphological and root physiological functions in heavily saline-sodic paddy soil of northeast China. *BioResources* **2022**, *17*, 1421–1456. [CrossRef]
31. Farhangi-Abriz, S.; Torabian, S. Antioxidant enzyme and osmotic adjustment changes in bean seedlings as affected by biochar under salt stress. *Ecotoxicol. Environ. Saf.* **2017**, *137*, 64–70. [CrossRef] [PubMed]
32. Yao, T.X.; Zhang, W.T.; Gulaqa, A.; Cui, Y.F.; Zhou, Y.M.; Weng, W.A.; Wang, X.; Jin, F. Effects of peanut shell biochar on soil nutrients, soil enzyme activity, and rice yield in heavily saline-sodic paddy field. *J. Soil Sci. Plant Nutr.* **2021**, *21*, 655–664. [CrossRef]
33. Li, X.B.; Che, W.K.; Piao, J.L.; Li, X.; Jin, F.; Yao, T.X.; Li, P.Y.; Wang, W.; Tan, T.; Shao, X.W. Peanut Shell Biochar's Effect on Soil Physicochemical Properties and Salt Concentration in Highly Saline-Sodic Paddy Fields in Northeast China. *BioResources* **2022**, *17*, 5936–5957. [CrossRef]
34. Jin, F.; Piao, J.L.; Miao, S.H.; Che, W.K.; Li, X.; Li, X.B.; Shiraiwa, T.; Tanaka, T.; Taniyoshi, K.; Hua, S.; et al. Long-term effects of biochar one-off application on soil physicochemical properties, salt concentration, nutrient availability, enzyme activity, and rice yield of highly saline-alkali paddy soils: Based on a 6-year field experiment. *Biochar* **2024**, *6*, 40. [CrossRef]
35. Piao, J.L.; Che, W.K.; Li, X.; Li, X.B.; Zhang, C.B.; Wang, Q.S.; Jin, F.; Hua, S. Application of peanut shell biochar increases rice yield in saline-alkali paddy fields by regulating leaf ion concentrations and photosynthesis rate. *Plant Soil* **2022**, *483*, 589–606. [CrossRef]
36. Ran, C.; Gulaqa, A.; Zhu, J.; Wang, X.W.; Zhang, S.Q.; Geng, Y.Q.; Guo, L.Y.; Jin, F.; Shao, X.W. Benefits of biochar for improving ion contents, cell membrane permeability, leaf water status and yield of rice under saline–sodic paddy field condition. *J. Plant Growth Regul.* **2022**, *39*, 370–377. [CrossRef]
37. Bastías, E.I.; González-Moro, M.B.; González-Murua, C. Zea mays L. amylacea from the Lluta Valley (Arica-Chile) tolerates salinity stress when high levels of boron are available. *Plant Soil* **2004**, *267*, 73–84. [CrossRef]
38. Bates, L.S.; Waldren, R.P.; Teare, I.D. Rapid Determination of Free Proline for Water-Stress Studies. *Plant Soil.* **1973**, *39*, 205–207. [CrossRef]

39. Bradford, M.M. Rapid and sensitive method for quantitation of microgram quantities of protein utilizing principle of protein-dye binding. *Anal. Biochem.* **1976**, *72*, 248–254. [CrossRef]
40. Du, Y.L.; Zhao, Q.; Chen, L.R.; Yao, X.D.; Xie, F.T. Effect of Drought Stress at Reproductive Stages on Growth and Nitrogen Metabolism in Soybean. *Agronomy* **2020**, *10*, 302. [CrossRef]
41. Stewart, R.R.C.; Bewley, J.D. Lipid Peroxidation Associated with Accelerated Aging of Soybean Axes1. *Plant Physiol.* **1980**, *65*, 245–248. [CrossRef]
42. Wang, S.Y.; Jiao, H. Scavenging capacity of berry crops on superoxide radicals, hydrogen peroxide, hydroxyl radicals, and singlet oxygen. *J. Agric. Food Chem.* **2000**, *48*, 5677–5684. [CrossRef] [PubMed]
43. Velikova, V.; Yordanov, I.; Edreva, A. Oxidative stress and some antioxidant systems in acid rain-treated bean plants. *Plant Sci.* **2000**, *151*, 59–66. [CrossRef]
44. Omran, R.G. Peroxide Levels and the Activities of Catalase, Peroxidase, and Indoleacetic Acid Oxidase during and after Chilling Cucumber Seedlings. *Plant Physiol.* **1980**, *65*, 407–408. [CrossRef] [PubMed]
45. Nakano, Y.; Asada, K. Hydrogen peroxide is scavenged by ascorbate-specific peroxidase in spinach chloroplasts. *Plant Cell Physiol.* **1981**, *22*, 867–880. [CrossRef]
46. Qadir, M.; Ghafoor, A.; Murtaza, G. Use of saline–sodic waters through phytoremediation of calcareous saline–sodic soils. *Agric. Water Manag.* **2001**, *50*, 197–210. [CrossRef]
47. Wang, Y.; Lin, Q.M.; Liu, Z.Z.; Liu, K.S.; Wang, X.; Shang, J.Y. Salt-affected marginal lands: A solution for biochar production. *Biochar* **2023**, *5*, 21. [CrossRef]
48. Torabian, S.; Farhangi-Abriz, S.; Rathjen, J. Biochar and lignite affect H^+-ATPase and H^+-PPase activities in root tonoplast and nutrient contents of mung bean under salt stress. *Plant Physiol. Biochem.* **2018**, *129*, 141–149. [CrossRef]
49. Song, X.L.; Li, H.B.; Song, J.X.; Chen, W.F.; Shi, L.H. Biochar/vermicompost promotes Hybrid Pennisetum plant growth and soil enzyme activity in saline soils. *Plant Physiol. Biochem.* **2022**, *183*, 96–110. [CrossRef]
50. Zheng, H.; Wang, X.; Chen, L.; Wang, Z.Y.; Xia, Y.; Zhang, Y.P.; Wang, H.F.; Luo, X.X.; Xing, B.S. Enhanced growth of halophyte plants in biochar-amended coastal soil: Roles of nutrient availability and rhizosphere microbial modulation. *Plant Cell Environ.* **2018**, *41*, 517–532. [CrossRef]
51. Talbi, Z.O.; Slama, I.; Trabelsi, N.; Hamdi, A.; Smaoui, A.; Abdelly, C. Combined effects of salinity and phosphorus availability on growth, gas exchange, and nutrient status of *Catapodium rigidum*. *Arid. Land Res. Manag.* **2018**, *32*, 277–290. [CrossRef]
52. Hasanuzzaman, M.; Bhuyan, M.H.M.B.; Anee, T.I.; Parvin, K.; Nahar, K.; Mahmud, J.A.; Fujita, M. Regulation of Ascorbate-Glutathione Pathway in Mitigating Oxidative Damage in Plants under Abiotic Stress. *Antioxidants* **2019**, *8*, 384. [CrossRef] [PubMed]
53. Maurya, A.K. Oxidative Stress in Crop Plants. *Agron. Crops* **2020**, *3*, 349–380. [CrossRef]
54. Nadarajah, K.K. ROS Homeostasis in Abiotic Stress Tolerance in Plants. *Int. J. Mol. Sci.* **2020**, *21*, 5208. [CrossRef]
55. Zhao, M.; Liu, Q.; Zhang, Y.; Yang, N.; Wu, G.F.; Wang, W. Alleviation of osmotic stress by H_2S is related to regulated PLDα1 and suppressed ROS in Arabidopsis thaliana. *J. Plant Res.* **2020**, *133*, 393–407. [CrossRef]
56. Tran, H.T.; Hurley, B.A.; Plaxton, W.C. Feeding hungry plants: The role of purple acid phosphatases in phosphate nutrition. *Plant Sci.* **2010**, *179*, 14–27. [CrossRef]
57. He, K.; He, G.; Wang, C.P.; Zhang, H.P.; Xu, Y.; Wang, S.M.; Kong, Y.Z.; Zhou, G.K.; Hu, R.B. Biochar amendment ameliorates soil properties and promotes Miscanthus growth in a coastal saline alkali soil. *Appl. Soil Ecol.* **2020**, *155*, 103674. [CrossRef]
58. Huang, M.Y.; Zhang, Z.Y.; Zhu, C.L.; Zhai, Y.M.; Lu, P.R. Effect of biochar on sweet corn and soil salinity under conjunctive irrigation with brackish water in coastal saline soil. *Sci. Hortic.* **2019**, *250*, 405–413. [CrossRef]
59. Zhang, M.; Liu, Y.; Wei, Q.; Liu, L.; Gu, X.; Gou, J. Biochar-Based Fertilizer Enhances the Production Capacity and Economic Benefit of Open-Field Eggplant in the Karst Region of Southwest China. *Agriculture* **2022**, *12*, 1388. [CrossRef]
60. Obadi, A.; Alharbi, A.; Alomran, A.; Alghamdi, A.G.; Louki, I.; Alkhasha, A. Effect of Biochar Application on Morpho-Physiological Traits, Yield, and Water Use Efficiency of Tomato Crop under Water Quality and Drought Stress. *Plants* **2023**, *12*, 2355. [CrossRef]
61. Mehmood, S.; Ahmed, W.; Ikram, M.; Imtiaz, M.; Mahmood, S.; Tu, S.; Chen, D. Chitosan Modified Biochar Increases Soybean (*Glycine max* L.) Resistance to Salt-Stress by Augmenting Root Morphology, Antioxidant Defense Mechanisms and the Expression of Stress-Responsive Genes. *Plants* **2020**, *9*, 1173. [CrossRef] [PubMed]
62. Cuevas, J.; Daliakopoulos, I.N.; del Moral, F.; Hueso, J.J.; Tsanis, I.K. A Review of Soil-Improving Cropping Systems for Soil Salinization. *Agronomy* **2019**, *9*, 295. [CrossRef]
63. Su, R.; Zhang, Z.K.; Chang, C.; Peng, Q.; Cheng, X.; Pang, J.Y.; He, H.H.; Lambers, H. Interactive effects of phosphorus fertilization and salinity on plant growth, phosphorus and sodium status, and tartrate exudation by roots of two alfalfa cultivars. *Ann. Bot.* **2022**, *129*, 53–64. [CrossRef] [PubMed]
64. Li, Y.F.; Li, G.H. Mechanisms of straw biochar's improvement of phosphorus bioavailability in soda saline-alkali soil. *Environ. Sci. Pollut. Res.* **2022**, *29*, 47867–47872. [CrossRef]
65. Zhang, P.; Bing, X.; Jiao, L.; Xiao, H.; Li, B.X.; Sun, H.W. Amelioration effects of coastal saline-alkali soil by ball-milled red phosphorus-loaded biochar. *Chem. Eng. J.* **2022**, *431*, 133904. [CrossRef]
66. Yang, L.; Wu, Y.C.; Wang, Y.C.; An, W.Q.; Jin, J.; Sun, K.; Wang, X.K. Effects of biochar addition on the abundance, speciation, availability, and leaching loss of soil phosphorus. *Sci. Total Environ.* **2020**, *758*, 143657. [CrossRef]

67. Elgharably, A. Wheat response to combined application of nitrogen and phosphorus in a saline sandy loam soil. *Soil Sci. Plant Nutr.* **2011**, *57*, 396–402. [CrossRef]
68. Abbasi, G.H.; Akhtar, J.; Ahmad, R.; Jamil, M.; Anwar-ul-Haq, M.; Ali, S.; Ijaz, M. Potassium application mitigates salt stress differentially at different growth stages in tolerant and sensitive maize hybrids. *Plant Growth Regul.* **2015**, *76*, 111–125. [CrossRef]
69. Thomas, S.C.; Frye, S.; Gale, N.; Garmon, M.; Launchbury, R.; Machado, N.; Melamed, S.; Murray, J.; Petroff, A.; Winsborough, C. Biochar mitigates negative effects of salt additions on two herbaceous plant species. *J. Environ. Manag.* **2013**, *129*, 62–68. [CrossRef]
70. Usman, K. Effect of phosphorus and irrigation levels on yield, water productivity, phosphorus use efficiency and income of lowland rice in northwest Pakistan. *Rice Sci.* **2013**, *20*, 61–72. [CrossRef]
71. Xu, G.; Zhang, Y.; Sun, J.N.; Shao, H.B. Negative interactive effects between biochar and phosphorus fertilization on phosphorus availability and plant yield in saline sodic soil. *Sci. Total Environ.* **2016**, *568*, 910–915. [CrossRef] [PubMed]
72. Huang, M.; Zhang, Z.; Zhai, Y.; Lu, P.; Zhu, C. Effect of Straw Biochar on Soil Properties and Wheat Production under Saline Water Irrigation. *Agronomy* **2019**, *9*, 457. [CrossRef]
73. Mahmoud, E.; Ibrahim, M.; Abd El-Rahman, L.; Khader, A. Effects of Biochar and Phosphorus Fertilizers on Phosphorus Fractions, Wheat Yield and Microbial Biomass Carbon in Vertic Torrifluvents. *Commun. Soil Sci. Plant Anal.* **2018**, *50*, 362–372. [CrossRef]
74. Cao, N.; Zhi, M.L.; Zhao, W.Q.; Pang, J.Y.; Hu, W.; Zhou, Z.G.; Meng, Y.L. Straw retention combined with phosphorus fertilizer promotes soil phosphorus availability by enhancing soil P-related enzymes and the abundance of phoC and phoD genes. *Soil Tillage Res.* **2022**, *220*, 106390. [CrossRef]
75. Shi, W.; Ju, Y.Y.; Bian, R.J.; Li, L.Q.; Joseph, S.; Mitchell, R.G.D.; Munroe, P.; Taherymoosavi, S.; Pan, G.X. Biochar bound urea boosts plant growth and reduces nitrogen leaching. *Sci. Total Environ.* **2020**, *701*, 134424. [CrossRef]